

# Relative velocities in bi-disperse turbulent aerosols: simulations and theory

Akshay Bhatnagar,<sup>1,\*</sup> K. Gustavsson,<sup>2</sup> B. Mehlig,<sup>2</sup> and Dhrubaditya Mitra<sup>1,†</sup>

<sup>1</sup>*Nordita, KTH Royal Institute of Technology and Stockholm University, Roslagstullsbacken 23, 10691 Stockholm, Sweden*

<sup>2</sup>*Department of Physics, Gothenburg University, 41296 Gothenburg, Sweden*

We perform direct numerical simulations of a bi-disperse suspension of heavy spherical particles in forced, homogeneous, and isotropic three-dimensional turbulence. We compute the joint distribution of relative particle distances and longitudinal relative velocities between particles of different inertia. For a pair of particles with small difference in their inertias we compare our results with recent theoretical predictions [Meibohm *et al.* Phys. Rev. E **96** (2017) 061102] for the shape of this distribution. We also compute the moments of relative velocities as a function of particle separation, and compare with the theoretical predictions. We observe good agreement. For a pair of particles that are very different from each other – one is heavy and the other one has negligible inertia – we give a new theory to calculate their root-mean-square relative velocity. This theory also agrees well with the results of our simulations.

## I. INTRODUCTION

Here we are concerned with small but heavy particles moving in a turbulent flow. How frequently and at what speeds do such particles collide with each other in turbulence? This question plays a central role in attempting to understand collisions and coalescence of microscopic water droplets in turbulent clouds [1], and to understand the formation of planetesimals in proto-planetary disks [2–4]. The particles in these turbulent aerosols are small and collisions between them are few and far between, consequently fluctuations matter. To understand how the distribution of particle sizes changes as a function of time, it is therefore not sufficient to merely consider the average collision rate. To account for the fluctuations it is necessary to consider the joint distribution of particle separations and their relative velocities [5–7]. A mean-field like description based solely on the first moment of relative particle velocities neglects fluctuations and may therefore not be reliable.

Völk *et al.* [8–10] and others [11, 12] formulated *inertial-range* theories for relative velocities of particles, referring to particle separations in the inertial range of turbulence. A criticism of this approach is that the collisions between the particles happen deep inside the dissipation range when the particle sizes are much smaller than the Kolmogorov length,  $\eta$ . It has been observed in direct numerical simulations (DNS) that inertial-range theories for the moments of relative velocities [8–10] fail at small Stokes numbers [13] (the Stokes number is a dimensionless measure of the importance of particle inertia). The predictions of Ref. [12] for the far tail of the distribution of relative velocities between nearby identical particles assume large Stokes numbers and a well-developed inertial range. This is difficult to achieve in DNS, and therefore it remains to be determined under which circumstances the prediction may hold.

Gustavsson *et al.* [6, 14–16] developed a *dissipation-range* theory for the distribution of relative velocities of identical particles, when the collision radius – the sum of the particle radii – is in the dissipation range of turbulence. An asymptotic form of the distribution was obtained by matching two limiting cases and using that inertial particles of identical sizes distribute on a fractal attractor in phase space [6, 14]. The result is a non-Gaussian distribution, with power-law tails that reflect large fluctuations. The theory applies in the limit where the Stokes number is large enough for particles to detach from the streamlines of the flow. But since the theory [6, 14–16] neglects inertial-range fluctuations, it may require modifications at very large Stokes numbers where the particle separations explore the inertial range.

In the astrophysical literature, DNS results for the relative-velocity distribution were recently reported by Ishihara *et al.* [13], as well as by Pan and Padoan [17, 18]. These authors fit the distribution to stretched exponentials. This raises the question how universal the power-law tails predicted in Refs. [6, 14] are. For Stokes numbers of order unity, the power laws were clearly seen in DNS [19, 20].

The findings and open questions described above apply to identical particles. But to understand how the size distribution of particles in turbulent aerosols changes as a result of collisions and coalescences, the distribution for particles of different sizes (different Stokes numbers) is needed. Meibohm *et al.* [21] developed a *dissipation-range* theory for the distribution of relative velocities of particles that have different Stokes numbers, by analyzing a statistical model in the white-noise limit. The predictions of Ref. [21] have not been tested in DNS yet.

To understand the distribution of relative velocities in turbulent aerosols is an important problem to study – both in theory and in simulations – because it is hard to obtain direct measurements of droplet velocities in clouds, and quite impossible as far as grain velocities in proto-planetary disks are concerned. There are two laboratory experiments [22, 23] that have measured the distribution of relative velocities of micron-sized particles in turbulence, and their mean and root-mean square

\* akshayphy@gmail.com

† dhruba.mitra@gmail.com

values as functions of particle separations. Experimental limitations make it difficult to measure at which relative velocities particles actually collide in these experiments. For micron-sized particles this occurs at separations deep inside the dissipative range, at present outside the spatial resolution of the experiments.

It is therefore important to validate existing theories for collision velocities of particles in turbulence by comparison with results of DNS. This is the purpose of the present paper. It is organized as follows: in Section II we describe the model and details of the DNS. In Section III we summarize the key theoretical results of Refs. [14, 21]. In Section IV we present our DNS results for the relative velocities between particles with different Stokes numbers. We compare the DNS results for the joint probability distribution of relative velocities and separations with the theoretical predictions of Meibohm *et al.* [21]. The distribution is non-Gaussian. When the difference between the Stokes numbers is not too large, then the distribution exhibits power-law tails as predicted by theory. At small separations and relative velocities, the power law in relative velocities is cut off, it becomes a broad Gaussian (approximately uniform), verifying the new velocity scale  $V_c$  predicted by theory [21]. Also the distribution of separations becomes uniform for separations smaller than  $R_c$ . This scale was predicted in Refs. [24, 25]. We show how the scales  $V_c$  and  $R_c$  are related. Finally, we develop a new theory for the root-mean-square (RMS) relative velocities of particles when one of the particles has very small Stokes number. We find that the results from this theory are in accord with our simulations. We conclude in Section VI.

## II. NUMERICAL METHOD

### A. Particle dynamics

We describe the motion of a heavy particle in a turbulent flow by the Stokes model [26]:

$$\frac{d}{dt}\mathbf{x} = \mathbf{v}, \quad \frac{d}{dt}\mathbf{v} = \frac{1}{\tau}[\mathbf{u}(\mathbf{x}, t) - \mathbf{v}]. \quad (1)$$

Here  $\mathbf{x}$  and  $\mathbf{v}$  are the position and velocity of the particle, the characteristic response time of the particle is  $\tau$ . The response time depends upon the particle size,  $a$ . In the Stokes limit,  $\tau = (2\rho_p/9\rho)a^2/\nu$ . Here  $\rho_p$  and  $\rho$  are the mass densities of the particle and the fluid, and  $\nu$  is the kinematic viscosity. Finally  $\mathbf{u}(\mathbf{x}, t)$  is the flow velocity. This model assumes that the effect of gravitational acceleration is small compared to the acceleration due to the turbulent flow, fluid-inertia corrections are small, and both particle-particle interactions and Brownian diffusion of individual particles are ignored.

### B. Direct numerical simulation of turbulence

The flow velocity  $\mathbf{u}(\mathbf{x}, t)$  is determined by solving the Navier–Stokes equation

$$\frac{\partial}{\partial t}\rho + \nabla \cdot (\rho\mathbf{u}) = 0, \quad (2a)$$

$$\rho\frac{D}{Dt}\mathbf{u} = -\nabla p + \mu\nabla \cdot \mathbb{S} + \mathbf{f}. \quad (2b)$$

Here  $\frac{D}{Dt} \equiv \partial_t + \mathbf{u} \cdot \nabla$  is the Lagrangian derivative,  $p$  is the pressure of the fluid, and  $\rho$  is its density as mentioned above. The dynamic viscosity is denoted by  $\mu \equiv \rho\nu$ , and  $\mathbb{S}$  is the second-rank tensor with components  $S_{kj} \equiv \partial_k u_j + \partial_j u_k - \delta_{jk}(2/3)\partial_l u_l$  (Einstein summation convention). Here  $\partial_k u_j$  are the elements of the matrix  $\mathbb{A}$  of fluid-velocity gradients. We use the ideal gas equation of state with a constant speed of sound.

Our simulations are performed in a three-dimensional periodic box with sides  $L_x = L_y = L_z = 2\pi$  in code units. To solve Eqs. (2) we use the pencil code [27], which uses a sixth-order finite-difference scheme for space derivatives and a third-order Williamson-Runge-Kutta [28] scheme for time derivatives. The external force  $\mathbf{f}$ , which is a white-in-time, Gaussian, stochastic process concentrated on a shell of wavenumber with radius  $k_f$  in Fourier space [29], is integrated by using the Euler–Maruyama scheme [30]. Under the action of the force the flow attains a statistically stationary state where the average energy dissipation by viscous forces is balanced by the average energy injection by the external force,  $\mathbf{f}$ . The amplitude of the external force is chosen such that the Mach number,  $\text{Ma} \equiv u_{\text{rms}}/c_s$  is always less than 0.1, i.e., the flow is weakly compressible which has no important effect on our results; please see the discussion in Ref. [20], section II and Appendix A in Ref [20] for further details. The same setup has been used before in studies of scaling and intermittency in fluid and magnetohydrodynamic turbulence [31–33].

We introduce the particles into the simulation after the flow has reached a statistically stationary state. Initially, the positions of the heavy particles are random and statistically homogeneous with zero initial velocity. Then we simultaneously solve Eqs. (1) and (2). To this end we must interpolate the flow velocity to typically off-grid positions of the heavy inertial particles. We use a trilinear method for interpolation.

We define the Reynolds number by  $\text{Re} \equiv u_{\text{rms}}/(\nu k_f)$ , where  $u_{\text{rms}}$  is the root-mean-square velocity of the flow averaged over the whole domain and the kinematic viscosity  $\nu$ . The mean energy dissipation rate  $\varepsilon \equiv 2\nu\Omega$  where the enstrophy  $\Omega \equiv \langle \omega^2 \rangle$ , and  $\omega \equiv \nabla \times \mathbf{u}$  is the vorticity. The Kolmogorov length is defined as  $\eta \equiv (\nu^3/\varepsilon)^{1/4}$ , the characteristic time scale of dissipation is given by  $\tau_\eta = (\nu/\varepsilon)^{1/2}$  and  $u_\eta \equiv \eta/\tau_\eta$  is the characteristic velocity scale at the dissipation length scale. In what follows, unless otherwise stated, we use  $\eta$ ,  $\tau_\eta$ , and  $u_\eta$  to non-dimensionalize length, time, and velocity respectively. The large eddy turnover-time is given by  $T_{\text{eddy}} \equiv 1/(k_f u_{\text{rms}})$ . We define the Stokes number as  $\text{St} \equiv \tau/\tau_\eta$ ,

TABLE I. Parameters for our DNS runs with  $N^3$  collocation points:  $\nu$  is the kinematic viscosity,  $N_p$  is the number of particles,  $\text{Re} \equiv u_{\text{rms}}/(\nu k_f)$  is based on the forcing wavenumber  $k_f$ ,  $\epsilon$  is the mean rate of energy dissipation,  $\eta \equiv (\nu^3/\epsilon)^{1/4}$ , and  $\tau_\eta \equiv (\nu/\epsilon)^{1/4}$  are the Kolmogorov length and time scales respectively, and  $T_{\text{eddy}} \equiv 1/(u_{\text{rms}}k_f)$  is the large-eddy-turnover time. The Mach number  $\text{Ma} = u_{\text{rms}}/c_s \approx 0.1$ . In the table we quoted dimensionless numbers.

| $N$ | $N_p$  | $\text{Re}$ | $1/(k_f\eta)$ | $T_{\text{eddy}}/\tau_\eta$ |
|-----|--------|-------------|---------------|-----------------------------|
| 512 | $10^7$ | 89          | 14.28         | 2.21                        |

where  $\tau$  is the particle response time in Eq. (1). As mentioned in the Introduction, this parameter measures the importance of particle inertia.

It is important to note that the particles in our simulations are actually point particles. As particle-particle interactions are ignored there are no real collisions. As far as the numerical code is concerned, the particles are characterized by the time-scale  $\tau$  which determines the Stokes number. To estimate the radius of a particle from its Stokes number we have used typical values of the ratio of the density of the particle to the density of the background fluid that corresponds to water droplets in clouds [34]. To obtain collision velocities that corresponds to dust in proto-planetary disks one must use different value of the density ratio. Also, since the sizes of the dust grains are smaller than the mean-free-path of the gas [2, 3, 35], we must use a different expression for the particle response time. It is obtained by replacing the mean free path  $\ell$  in  $\nu = \ell c_s$  (where  $c_s$  is the sound speed) by the particle size  $a$ . This yields  $\tau \sim a$  instead of the quadratic dependence  $\tau \sim a^2$  in Stokes law.

### III. THEORETICAL BACKGROUND

In this Section we summarize the dissipation-range theory for the distribution of relative velocities between two particles with different Stokes numbers [21]. We denote the relative-particle velocity by  $\mathbf{V} = \mathbf{v}_2 - \mathbf{v}_1$ , where  $\mathbf{v}_1$  and  $\mathbf{v}_2$  are the individual particle velocities. The distance between the particles is denoted by  $R = |\mathbf{R}|$ , where  $\mathbf{R} = \mathbf{x}_2 - \mathbf{x}_1$  is the separation vector between the particle positions, and the longitudinal relative velocity is defined as  $V_R = \mathbf{V} \cdot \mathbf{R}/R$ . We denote the steady-state distribu-

tion of relative velocities and separations by  $\mathcal{P}(R, V_R)$ . The moments of the distribution are characterized by

$$\langle |V_R|^p \rangle \equiv \frac{m_p(R)}{m_0(R)}, m_p(R) = \int dV_R |V_R|^p \mathcal{P}(R, V_R). \quad (3)$$

The factor  $m_0(R)$  is related to the pair correlation function by  $m_0(R) \propto g(R)R^{d-1}$  [6].

#### A. Distribution of relative velocities and separations

Gustavsson and Mehlig [6, 14, 15] developed a theory for the distribution of relative velocities of nearby *identical* particles. The theory takes into account particle inertia, and it rests on the observation that such particles form fractal spatial patterns in turbulence [26], and that caustics can give rise to large relative velocities at small separations [36–38]. The theory predicts that the distribution of relative velocities  $V_R$  at small separations  $R$  is a power law, reflecting fractal clustering in phase space. The power-law exponent is related to the phase-space correlation dimension  $D_2$  [6, 14, 21]. The distribution determines the scaling of relative-velocity moments (3) with separation  $R$  [15]. These predictions for *identical* particles should hold for turbulence as well as statistical-model flows. In the white-noise limit, the theory was derived from first principles in Refs. [6, 14]. For turbulent flows, the theoretical predictions were verified using DNS [19, 20, 39] and using kinematic turbulence simulations [15]. See also Refs. [40–43].

The correlation dimension  $D_2$  is not universal. In the white-noise limit  $D_2$  can be calculated in perturbation theory [14, 26], but in general it must be determined numerically. As is well known,  $D_2$  depends non-monotonically on  $\text{St}$  with a minimum at  $\text{St}$  of order unity [44].

Particles with *different* Stokes numbers cluster on distinct fractal attractors, so that the distribution of separations between particles with different Stokes numbers is cut off at a small spatial scale,  $R_c$  that depends on the difference between the Stokes numbers [24, 25]. How are the relative velocities of nearby particles affected? In Ref. [21] a statistical model for relative velocities between particles with different Stokes numbers was analyzed in the white-noise limit. It was shown that there is a new velocity scale  $V_c$ , and that the distribution of  $V_R$  and  $R$  is a broad Gaussian below these scales [21], in other words approximately uniform:

$$\mathcal{P}(R, V_R) = \mathcal{N} R^{d-1} \begin{cases} 1 & \text{for } |V_R| < V_c \text{ and } R < V_c/z^*, \\ R^{\mu_c-d-1} & \text{for } R > V_c/z^* \text{ and } |V_R| < z^*R, \\ (|V_R|/z^*)^{\mu_c-d-1} & \text{for } |V_R| > V_c \text{ and } z^*R < |V_R|, \\ 0 & \text{for } |V_R| > V_0. \end{cases} \quad (4)$$

In addition to the normalization  $\mathcal{N}$  there are four more

parameters in Eq. (4): the two velocity scales  $V_c$  and  $V_0$ ,

the power-law exponent  $\mu_c$ , and the parameter  $z^*$ .

The last parameter,  $z^*$ , defines the line  $|V_R| = z^*R$  in the  $R$ - $V_R$  plane where known limiting behaviors of  $\mathcal{P}(R, V_R)$  in the dissipative range are matched to obtain the theoretical predictions for  $\mathcal{P}(R, V_R)$ .

The exponent  $\mu_c$  is related to the phase-space correlation dimension  $D_2(\overline{\text{St}})$  of the mono-disperse system with Stokes number  $\overline{\text{St}}$

$$\mu_c = \min\{D_2(\overline{\text{St}}), d + 1\}, \quad (5)$$

where  $d = 3$  is the spatial dimension, and  $\overline{\text{St}}$  is the harmonic mean of the two Stokes numbers,

$$\overline{\text{St}} = \frac{2\text{St}_1\text{St}_2}{\text{St}_1 + \text{St}_2}. \quad (6)$$

The parameter  $D_2$  can be calculated analytically in the white-noise limit [21, 45, 46], but in turbulent flows it must be determined numerically.

Now consider the upper velocity scale  $V_0$ . It was assumed in deriving Eq. (4) that it suffices to consider separations in the dissipative range where the turbulent fluid velocities are spatially smooth. This range extends up to separations  $R$  somewhat larger than the Kolmogorov length  $\eta$ . The theory mirrors the distribution of spatial separations for  $R < 1$  to distributions in relative velocities, just as it does for identical particles. Therefore the upper cutoff for the  $V_R$  power laws is

$$V_0 = z^*. \quad (7)$$

How this parameter depends upon the Stokes number is not known in general. In a one-dimensional statistical model this parameter was calculated in the white-noise limit in Ref. [6].

In Eq. (7), the distribution was simply set to zero for  $V_R > V_0$ . This is an oversimplification, in particular for turbulence where the far tails of the  $V_R$ -distribution at small spatial separations result from particle pairs that have had separations in the inertial range in the past. For large Stokes numbers and when the inertial range is well developed it was argued in Ref. [12] that the tail of the conditional distribution  $\mathcal{P}(R=0, V_R)$  has the form  $\sim C_1/(\varepsilon\tau)^{1/2} \exp[-C_2|V_R|^{4/3}/(\varepsilon\tau)^{2/3}]$  for very large Stokes numbers. A statistical-model calculation with an inertial range yields the prefactors  $C_1$  and  $C_2$  in the white-noise limit, but they could have different parameter dependencies in turbulence [47]. At smaller  $\text{Re}$ , when the inertial range is not well developed, one may argue that the tail should be well approximated by a Gaussian with variance  $\propto u_{\text{rms}}^2$ . The RMS turbulent velocity is an estimate of the relative velocities of particles that move independently at large separations, of the order of the system size. In summary, the far tail of the relative-velocity distribution is not universal. Here we simply set

$$V_0 = u_{\text{rms}} \quad (8)$$

when we compare with our DNS data.

The fourth parameter in Eq. (4) is the scale  $V_c$ . It depends upon the difference of the two Stokes numbers. We follow Ref. [21] and write

$$\theta = \frac{|\text{St}_1 - \text{St}_2|}{\text{St}_1 + \text{St}_2}. \quad (9)$$

The white-noise model predicts that [21]

$$V_c \propto \theta \quad (10)$$

at small  $\theta$ . In this case, the power-law tails of the distribution (4) are expected to contribute to the relative velocity moments. According Eq. (4), the tails of the distribution beyond  $V_c$  are simply those of the mono-disperse system.

Eq. (4) implies that the distribution of separations becomes uniform in  $R$  for  $R < R_c$ , as predicted in Refs. [24, 25]. Their spatial scale  $R_c$  is thus related to our velocity scale as follows:

$$R_c \equiv V_c/z^*, \quad (11)$$

and therefore  $R_c \propto \theta$  at small  $\theta$ .

## B. Moments of relative velocities

Theoretical predictions for  $\langle |V_R|^p \rangle$  are obtained by integrating the distribution  $\mathcal{P}$ , as determined by Eq. (3). We first quote the results when  $\theta$  is small, when the distribution exhibits a clear power law. This power law is cut off at small relative velocities at  $\max(V_c, z^*R) = z^*\max(R_c, R)$ , consequently the result for  $\langle |V_R|^p \rangle$  depends on whether  $R > R_c$  or not. When  $R > R_c$  we find

$$m_p(R) = b_p R^{\mu_c + p - 1} + c_p R^{d - 1}, \quad (12)$$

with

$$b_p = -\frac{\mathcal{N}(1+d-\mu_c)z^{*p+1}}{(p+1)(\mu_c-d+p)}, \quad (13)$$

$$c_p = \frac{\mathcal{N}z^{*p+1}\left(\frac{V_0}{z^*}\right)^{\mu_c-d+p}}{\mu_c-d+p},$$

where  $\mathcal{N}$  is the normalization factor in Eq. (4). For large values of  $p$ , the coefficients  $b_p$  and  $c_p$  are sensitive to the form of the distribution beyond the cutoff  $z^*$ , which depends on the nature of the turbulent fluctuations. Also, the value of  $\mu_c = D_2(\overline{\text{St}})$  is not universal, and neither is the parameter  $z^*$ . The second term in Eq. (12) appears due to presence of singularities (of the gradient of particle velocity) called caustics [37, 38] for non-zero values of  $\text{St}$ . In other words, the presence of caustics imply that while the distance between two nearby particles goes to zero their relative velocities can remain order unity. Whereas, in the absence of caustics, the particle velocity field remains smooth – relative velocity of two particles

goes to zero as separation between them goes to zero, this gives rise to first term in Eq. (12) (see Ref. [6] for more discussion).

The  $R$ -dependence predicted by Eq. (12) is universal. It is equal to the scaling form of  $m_p(R)$  for identical particles [15], as expected for small  $\theta$ . But for particles with different Stokes numbers the coefficients  $b_p$  and  $c_p$  depend upon  $\theta$ , although only through the global normalization constant  $\mathcal{N}$ . The scale  $V_c$  does not enter explicitly because  $R > R_c$ .

Now consider  $R < R_c$ . Then the uniform part in Eq. (4) dominates the moments. At  $R < R_c$ , particles of two different sizes  $a_1$  and  $a_2$  move approximately independently from each other. In this case the moments take the form:

$$m_p(R) \sim c'_p R^{d-1}, \quad (14)$$

with

$$c'_p = c_p - \frac{\mathcal{N}(1+d-\mu_c)(V_c/z^*)^{\mu_c-d+p} z^{*p+1}}{(\mu_c-d+p)(p+1)}. \quad (15)$$

For  $p = 1, 2, 3, \dots$  one finds that  $c'_p < c_p$  for heavy particles in incompressible turbulence at not too large Stokes numbers [DNS show that  $D_2 > d-1$ , and that  $D_2 < d+1$  for not too large Stokes numbers, see Eq. (5)]. The moments for larger  $\theta$  are nevertheless usually larger than those for  $\theta \rightarrow 0$ , because the term  $b_p R^{D_2+p-1}$  makes a large negative contribution unless  $R$  is extremely small, and this term is absent in Eq. (14). In general, if  $\overline{St}$  is small enough so that caustics are rare, then Eq. (14) can give a contribution for different particles that is much larger than for identical particles, leading to a significantly higher collision rate. The dependence on  $R$  is of the same form as the caustic contribution in Eq. (3) in the limit  $\theta \rightarrow 0$ .

Finally consider larger values of  $\theta$ , large enough so that the power laws in Eq. (4) disappear. In a Gaussian white-noise model the distribution  $\mathcal{P}(R, V_R)$  is Gaussian in this limit [21].

### 1. Very dissimilar pair of particles

When one of the particles has a very small Stokes number,  $St_2 \ll 1$  say, we can evaluate the coefficient  $c'_p$  term in Eq. (14) in terms of single-particle observables. We now outline the calculation for  $p = 2$ . When  $St_2 \ll 1$ , we can expand the equation of motion up to leading order in  $St_2$  to obtain the velocity of the second particle:

$$\mathbf{v}_2 \approx \mathbf{u}(\mathbf{x}, t) - \mathbb{A} \cdot \mathbf{R} - St_2 \frac{D\mathbf{u}}{Dt}(\mathbf{x} + \mathbf{R}, t). \quad (16)$$

The relative velocity between two particles can then be written as

$$\mathbf{V}(\mathbf{R}) \approx \mathbf{v} - \mathbf{u}(\mathbf{x}, t) + \mathbb{A} \cdot \mathbf{R} + St_2 \frac{D\mathbf{u}}{Dt}(\mathbf{x} + \mathbf{R}, t). \quad (17)$$

The first line of the right-hand-side of Eq. (17) is  $St_1$  times the acceleration of a *single* particle; at small  $|\mathbf{R}|$  and  $St_2$  this is the leading order contribution to the relative velocity. The distribution of the acceleration has been studied extensively and is known to have exponential tails [48, 49]. This information allows us to approximately relate the structure functions to single-particle averages, as shown below.

We assume that to calculate  $\langle V_R^2 \rangle$  for  $R$  much smaller than  $R_c$  it is sufficient to consider one component of  $\mathbf{V}$ . Consider one component of Eq. (17), square both sides of the resultant equation and then take steady-state averages. Assuming that  $R \ll 1$  we obtain:

$$\langle V_R^2 \rangle \approx \frac{1}{3} [\langle \mathbf{u}^2 \rangle - \langle \mathbf{v}^2 \rangle] \left( 1 - 2 \frac{St_2}{St_1} \right) - \frac{2}{3} St_2 \langle (\mathbf{u} - \mathbf{v}) \cdot \mathbb{A} \cdot (\mathbf{u} - \mathbf{v}) \rangle. \quad (18)$$

All averages on the r.h.s. of Eq. (18) are evaluated for a single particle with Stokes number  $St_1$ . The only  $St_2$ -dependence appears in the prefactors on the r.h.s. of Eq. (18). We note that there is no  $R$ -dependence (since all averages are single-particle averages). This is the result of neglecting the gradient term  $\mathbb{A} \cdot \mathbf{R}$  in the equation for the particle separations. As explained in Section II.A of Ref. [21] this is allowed provided that  $R < R_c$ . But note that in Ref. [21] the *white-noise model* was analyzed, while Eq. (18) applies to a turbulent flow.

## IV. DNS RESULTS

### A. Distribution of relative velocities and separations

Fig. 1 shows a comparison between the theory Eq. (4) and our DNS results for  $\mathcal{P}(R, V_R)/R^2$  for different values of  $\theta$ . The first column of panels in this Figure shows contour plots of  $\mathcal{P}(R, V_R)/R^2$ . As predicted by the theory (4), there is a region in the  $R$ - $V_R$  plane where the distribution is a broad Gaussian. In a log-log plot this appears as an approximately uniform region where  $\mathcal{P}/R^2$  is approximately constant. Outside this region, and for small values of  $\theta$ , the equidistant contour lines show that the distribution exhibits the power laws, as predicted by the theory.

To analyze the power laws in relative velocities in more detail, the second column of panels in Fig. 1 shows plots of  $\mathcal{P}(R, V_R)/R^2$  as functions of  $|V_R|$  for several different values of  $R$ . We can clearly distinguish the power-law from the broad Gaussian at small  $|V_R|$ , where  $\mathcal{P}/R^2 \approx \text{const}$ . Eq. (4) says that the cross over between these two behaviors occurs at  $\min(V_c, z^* R)$ . We estimate this cross-over velocity scale by drawing two lines: a horizontal one at small  $|V_R|$ , and a power-law fit for larger  $|V_R|$ . The scale at which these two lines intersect is our estimate of the cross-over scale. For small values of  $R$  the fits yield a velocity scale that is independent of  $R$ , this is

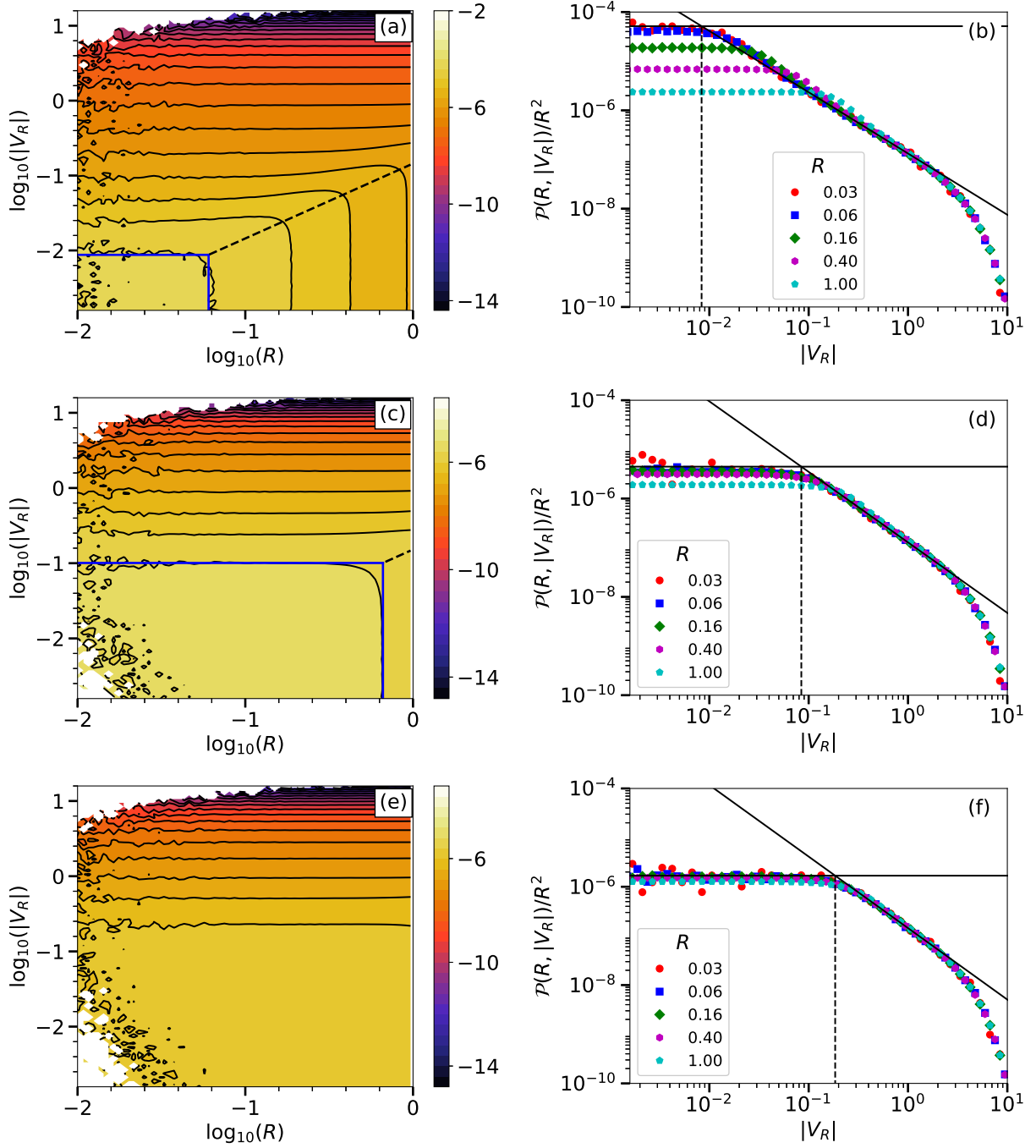


FIG. 1. (color online) DNS results for joint distribution  $\mathcal{P}(R, |V_R|)$  of  $R$  and  $|V_R|$ , divided by  $R^2$ . Parameters:  $\overline{\text{St}} = 2$  and  $\theta = 0.005$  (top row),  $\theta = 0.05$  (second row), and  $\theta = 0.1$  (bottom row). First column: Contour plots of  $\mathcal{P}(R, |V_R|)/R^2$  color coded according to  $\log_{10}[\mathcal{P}(R, |V_R|)/R^2]$ . The blue lines in the bottom left corner of these plots show the scales  $R_c$  and  $V_c$  (see text). The dashed lines show the theoretical matching condition  $|V_R| = z^* R$  (see text). Second column: plots of  $\mathcal{P}(R, |V_R|)/R^2$  as functions of  $|V_R|$  for different values of  $R$  as indicated in the panels. Also shown are fits (solid lines) to the theoretical power-law prediction  $|V_R|^{\mu_c - 4}$ , Eq. (4), to determine  $\mu_c$  as a function of  $\text{St}$ . The crossover between the approximately uniform (broad Gaussian) part at small  $|V_R|$  and small  $R = 0.03, 0.06$ , horizontal solid lines) and the power-law at intermediate  $R$  sets the scale  $V_c$  (dashed vertical lines).

$V_c$ . For slightly larger values of  $R$ , the velocity scale is proportional to  $R$ , as predicted by theory, and the constant of proportionality defines the parameter  $z^*$ .

Dissipation-range theory [21] says that  $V_c = c\theta$  for small  $\theta$ , but the theory does not determine the constant of proportionality  $c$ . This constant is system specific, as is the value of  $z^*$ . In the white-noise limit these parameters can be calculated analytically [6, 21], but not in general.

Therefore it is important to determine these constants by DNS. The results are shown in Fig. 2. Panel (a) shows that  $z^*$  is essentially independent of  $\theta$ , while panel (b) demonstrates that  $V_c$  is proportional to  $\theta$  at small  $\theta$ , as predicted by the theory. Fig. 2(b) also shows that the prefactor depends on  $\overline{St}$  as  $\overline{St}^{1/2}$ , at least for the parameters simulated. This follows from the fact that the DNS data for  $V_c \overline{St}^{-1/2}$  collapse onto a single line. However, there is no theoretical explanation for this result, as far as we know.

Fig. 2(c) shows the power-law exponents  $\mu_c$ . We extracted  $\mu_c$  for different values of  $\overline{St}$  and for two different values of  $\theta$  by fitting power laws to the DNS results for the distribution of relative velocities. Panel (c) shows the resulting exponents  $\mu_c$  together with  $D_2$  for the case  $St_1 = St_2$  from Ref. [20]. Up to the numerical accuracy in our DNS we find for  $D_2 < 4$  that  $\mu_c = D_2$ , independent of  $\theta$  for small values of  $\theta$ . The phase-space correlation dimension  $D_2$  has a characteristic minimum at  $\overline{St}$  of order unity and monotonously approaches the spatial dimension  $d$  for small  $\overline{St}$  and the dimensionality of phase space,  $2d$ , for large  $\overline{St}$  [see Fig. 2(c)].

In summary we observe good agreement between our DNS and the theory, Eq. (4), in particular for small  $\theta$ . As  $\theta$  increases, the velocity scale  $V_c$  grows so that the range of the power law between  $V_c$  and  $V_0$  becomes smaller. For large enough values of  $\theta$ , the power laws disappear. In this limit the distribution is a broad Gaussian, approximately uniform. In our log-log plots,  $\mathcal{P}/R^2$  is approximately constant in this region.

## B. Moments of relative velocities

Fig. 3 summarizes our DNS results for the moments of relative velocities as a function of particle separation. Panel (a) shows DNS results for  $m_0(R)/R^2$  as a function of  $R$  (symbols), while panel (b) shows  $m_2(R)/R^2$ , also as a function of  $R$ . The parameters are given in the Figure caption. Also shown is the scaling of the smooth contribution predicted by Eq. (12) (solid line). Dashed vertical lines correspond to the scale  $R_c = V_c/z^*$ . The parameters  $V_c$ ,  $\mu_c$ , and  $z^*$  were determined separately, as described in Section IV A.

As predicted by Eq. (12), the moments scales as  $R^{d-1}$  for  $R < R_c$ . For  $R > R_c$  smooth contribution dominates for  $m_0(R)$  for both values of  $\overline{St}$ , whereas for higher order moment  $m_2(R)$  smooth contribution dominates only for the smaller mean Stokes number. For larger mean Stokes number, the caustic contribution  $c_p R^{d-1}$  swamps

the smooth part for  $R$  below  $R_c$ . In limit the relative-velocity moments  $m_p(R)$  are dominated by the singular  $R^{d-1}$ -contribution provided that  $p$  is large enough. While the  $R$ -dependence of this contribution is the same for identical particles and for particles with different Stokes numbers, the physical origin of this power law is slightly different in the two cases. For identical particles, the singular term is caused by caustics [36–38]. For particles with different Stokes numbers, by contrast, the singular contribution is due to the uncorrelated motion between nearby ( $R < R_c$ ) particles with different Stokes numbers [21].

### 1. Very dissimilar pair of particles

Fig. 3(c) shows DNS results for  $\langle V_R^2 \rangle$  at the collision radius  $R = a_1 + a_2$  for  $St_2 \ll 1$  as a function of  $St_1$  (red circles), that is for large values of  $\theta$ . Also shown is the theoretical expression, Eq. (18) (green squares). The averages on the r.h.s. of Eq. (18) are determined by DNS, by averaging along heavy-particle paths in the steady state. The agreement is good at small values of  $St_1$ , but we observe deviations at larger values of the Stokes number. It is possible that this is due to higher- $St_2$ -terms neglected in (18). Plotting only the first term of Eq. (18) yields slightly different results, although the deviations are smaller than those between the full theory and the DNS results.

We have checked that the gradient term  $\mathbf{A} \cdot \mathbf{R}$  in the equation of motion for the separation  $\mathbf{R}$  is negligible. For all data points shown,  $\theta$  is large enough so that  $a_1 + a_2$  is much less than  $R_c$ . In this range the DNS results do not depend upon  $R$ . This is the plateau region seen in Fig. 3(a).

## V. DISCUSSION

Our results show in agreement with the theory that the distribution of relative velocities is non-Gaussian when  $\theta$  is small. For a fairly wide range of  $\theta$  (up to  $\theta \sim 0.1$ ), the distribution has power-law tails  $\sim |V_R|^{\mu_c-4}$  at small separations. The dissipation-range theory predicts that the exponent  $\mu_c$  is determined by the *phase-space* correlation dimension  $D_2(\overline{St})$  for a mono-disperse system with Stokes number  $\overline{St}$  [Eq. (5)]. In our simulations, the numerical values of  $\mu_c$  vary from approximately 2.4 to 3.5, and in this range there is good agreement between the theory and the numerical values of  $\mu_c$  obtained from the DNS [50].

In the astrophysical literature, several papers have reported DNS results for the distribution of relative particle velocities [13, 17, 18]. These authors attempted to fit the distributions to stretched exponentials, of the form  $\exp[-(|V_R|/\beta)^\gamma]$  with fitting parameters  $\beta$  and  $\gamma$ . The parameter  $\gamma$  is usually quoted to be smaller than unity. This law is neither consistent with our power-law predic-

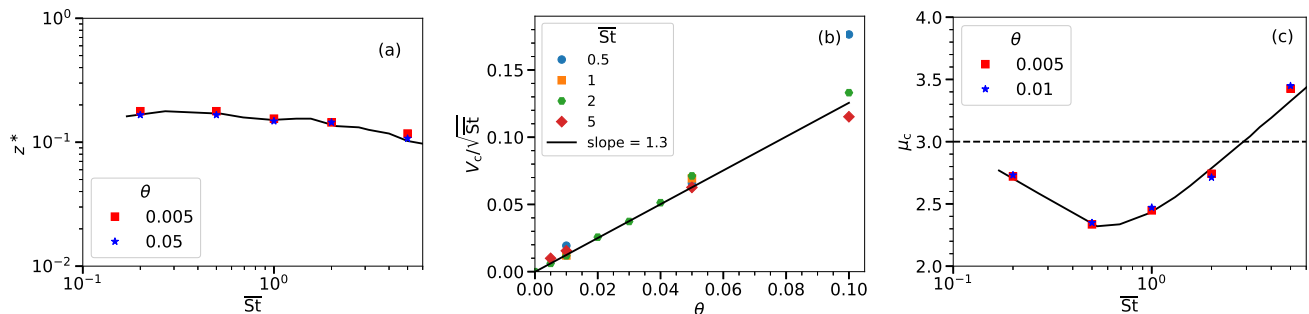


FIG. 2. (color online) Estimates of the parameters  $z^*$ ,  $V_c$ , and  $\mu_c$ , obtained from the DNS results for  $\mathcal{P}(R, V_R)$  shown in Fig. 1. (a) Scale  $z^*$  as a function of  $\overline{St}$ , for two different values of  $\theta$  (symbols). The solid black line is the estimate for identical particles, taken from the DNS of Ref. [20]. (b) Scale  $V_c$  as a function of  $\theta$  (symbols), for different values of  $\overline{St}$ . The solid black line shows a linear dependence upon  $\theta$  with fitted prefactor 1.3. (c) Exponent  $\mu_c$  as a function of  $\overline{St}$  for two different values of  $\theta$  obtained by power-law fits to DNS results for  $\mathcal{P}(R, V_R)$  at fixed  $R$ , see Fig. 1. The solid black line is the phase-space correlation dimension  $D_2$  of the fractal attractor for identical particles with Stokes number  $\overline{St}$ , taken from Ref. [20].

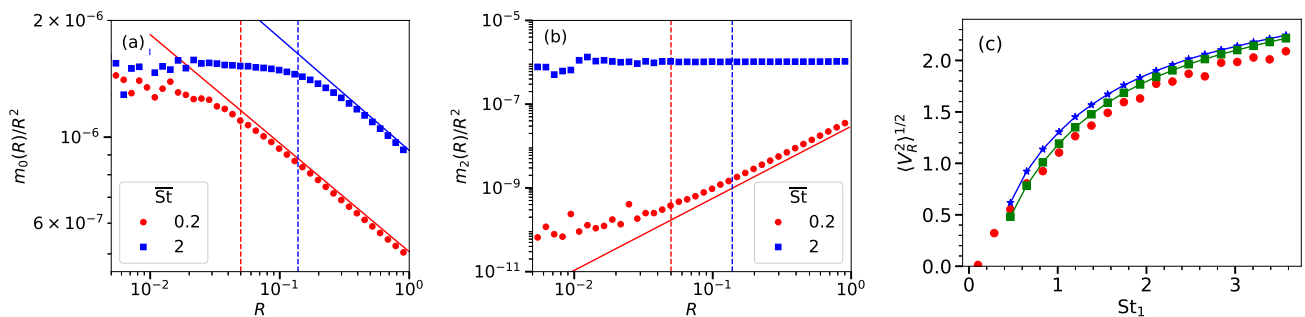


FIG. 3. (color online) DNS results for moments of relative velocities as a function of particle separation  $R$ . (a) Zero-th moment  $m_0(R)$  and (b) second moment divided by  $R^2$ , for  $\overline{St} = 0.2$  and  $2$ , and  $\theta = 0.01$  (symbols). Solid line shows the scaling of smooth contribution in Eq. (12). The scale  $R_c = V_c/z^*$  is indicated by the dashed vertical line. (c) Root-mean-square radial velocity  $\langle V_R^2 \rangle^{1/2}$  for  $R = a_1 + a_2$  plotted as a function of  $St_1$  for  $St_2 = 0.1$  (red circles). The first term of theoretical estimate, Eq. (18), is plotted as blue  $\star$  (joined with a blue solid line). The full expression Eq. (18), is plotted with green  $\blacksquare$  (joined by a green solid line).

tions, nor with the large- $St$  prediction from Ref. [12]. We have reanalyzed the data in Fig. 12 of Ref. [13] for the two smallest Stokes numbers, and find clear power laws over one decade of  $V_R/u_\eta$ , with exponents  $\mu_c - 4$  in good agreement with the dissipation-range theory (the values of  $\mu_c$  were obtained from the plots of the pair correlation function in Fig. 8 of the same paper).

We remark that the distribution of relative velocities in bidisperse suspensions was recently studied in Ref. [51]. This study did not report power-laws for the distribution of relative velocities. As our results show, possible reasons for the absence of power laws are, firstly, that the distributions were calculated at quite large separations (of the order of the Kolmogorov length,  $R \sim \eta$ ). Secondly, the values of  $\theta$  were quite large, too large to see power laws as our theory and DNS data demonstrate.

Pan and Padoan [17] did not plot the radial relative velocity  $V_R$  (that determines how particles approach each other), but instead the RMS relative velocity  $V_{\text{rms}} \equiv$

$\sqrt{V_1^2 + V_2^2 + V_3^2}$ . The power law of the distribution of  $V_{\text{rms}}$  has a different exponent [6, 14]:  $|V_{\text{rms}}|^{\mu_c - 2d}$ . We have compared this prediction with the data shown in Fig. 14 of Ref. [17]. There is a clear power law, with exponent  $\approx -3.7$  for  $St = 1.55$ . Theory says that the exponent should equal  $D_2 - 6$ , but Ref. [17] does not give values for the fractal correlation dimension  $D_2$ . Estimating  $D_2$  from our data at  $St = 1.55$  (albeit at a different Reynolds number), we find  $D_2 - 6 \approx -3.4$ , in reasonable but not perfect agreement with the DNS results of Ref. [17].

Ishihara *et al.* state that their distribution approaches a Gaussian when  $\theta$  is not small. This is consistent with theory [21], predicting a broad Gaussian for the body of the distribution. In our log-log plots, Fig. (1), the broad Gaussian appears as a region where  $\mathcal{P}/R^2$  is approximately constant. When  $\theta$  is large enough, this region extends out to  $V_0$ , approximately equal to the RMS turbulent velocity,  $u_{\text{rms}}$ . The form of the far tails beyond



$V_0$  is difficult to determine, because the tails describe rare events, and since there is no theoretical prediction apart from the law predicted in Ref. [12]. Yet this applies only at large Stokes numbers, and when there is a well-developed inertial range.

In both cases, when  $\theta$  is small and when it is large, the RMS relative velocity is determined by the upper cutoff,  $V_0$ . We have simply set  $V_0 = u_{\text{rms}}$  here, but this is a simplification. In general, the upper cutoff  $V_0$  must also depend on particle inertia (Stokes number). We have neglected this dependence here. Taking  $V_0 = u_{\text{rms}}$  implies that the moments of particle relative velocities depend on the Reynolds number  $\text{Re}$  when determined by the upper cutoff  $V_0$ , since  $u_{\text{rms}}/u_\eta \propto \text{Re}^{1/4}$  [52]. With our present computational capabilities we cannot explore such a weak dependence on  $\text{Re}$ ; hence we have concentrated our efforts on a single value of  $\text{Re}$ . Experimental data [23] confirms that the  $\text{Re}$ -dependence is quite weak.

Ishihara *et al.* [13], on the other hand, computed RMS relative particle velocities for different values of  $\text{Re}$  (Fig. 3 in their paper), obtaining a fairly strong dependence on  $\text{Re}$ . A possible explanation of this result is that Ishihara *et al.* evaluated  $\langle V_R^2 \rangle$  at fixed separation  $r = 10^{-3}L$ . Changing  $\text{Re}$  while keeping the system size  $L$  the same changes the Kolmogorov length  $\eta$  and hence  $R = r/\eta$  is different for different value of  $\text{Re}$ . Unless  $R < R_c$  (whether this condition is satisfied or not is determined by the values of the Stokes numbers), the relative velocity statistics depends on  $R$ , as the dissipation-range theory shows. Thus evaluating the moments at  $r = 10^{-3}L$  for changing  $\eta$  may give rise to a spurious  $\text{Re}$  dependence. It would be of interest to test quantitatively whether the  $\text{Re}$ -dependence predicted by the dissipation-range theory is consistent with this explanation.

It is a strength of the dissipation-range theory summarized in Section III that it predicts how the moments of relative velocities depend upon particle separation  $R$ . The microscopic dust grains in accretion disks are much smaller than the Kolmogorov length  $\eta$ , so that the collision radius  $R = a_1 + a_2$  is well below  $\eta$ . Inertial-range theories [8–12] do not refer to scales below  $\eta$ . As a consequence they cannot describe collisions that occur deep in the dissipation range. In DNS it is also difficult to reach to such small scales, much smaller than  $\eta$ , simply because particles rarely come so close. But collisional aggregation in turbulent aerosols is fluctuation dominated when the systems are dilute, so that such rare events matter. Several recent works [13, 17, 53] give results for RMS relative velocities at fixed separations, usually of order  $\eta$ , irrespective of the size of the particles. The theory (12-15) allows to extrapolate the DNS results to  $R = a_1 + a_2$ . Here the parameter  $R_c = V_c/z^*$  plays an important role. If  $R < R_c$  then the theory shows that the relative particle-velocity statistics is independent of the separation  $R$ .

A weakness of the dissipation-range theory is that it expresses the prefactors  $b_p$  and  $c_p$  in the  $R$ -dependence of the moments in terms of parameters  $z^*$ ,  $\mu_c$ ,  $V_c$ , and  $V_0$

that must be determined separately, by DNS for example. The theory shows, moreover, that the prefactors are not universal. It would therefore be of great interest to find alternative ways of computing these prefactors. One possibility, although numerical, is to use the approach of Zaichik and collaborators [54, 55] and its refinements [56].

## VI. SUMMARY AND CONCLUSIONS

Let us summarize the key findings here. We used direct numerical simulations of particle-laden, homogeneous and isotropic, forced turbulence to study the statistics of relative velocities and separations between particles with different Stokes numbers. We computed the joint distribution of particle separations and their relative velocities. We found that the shape of the distribution is in good agreement with the predictions of dissipation-range theory [21]. When the difference between the two Stokes numbers is small enough, then the distribution exhibits power laws, and the exponent is related to fractal patterns in phase space [26]. We found that the power laws are cut off at small relative velocities, at a scale  $V_c$ . We found that  $V_c$  depends linearly on  $\theta$  for small values of  $\theta$ , in agreement with the theoretical prediction [21].

When  $\theta$  is large, by contrast, theory predicts that the body of the distribution is broad Gaussian [21], in agreement with the DNS of [13, 53]. In a log-log plot Fig. 1 this Gaussian appears as a region where  $\mathcal{P}/R^2$  is roughly constant. The shape of the distribution beyond  $V_0$  (here simply set to zero) is not known. There are indications [53] that the theory of Ref. [12] may work for the tails. But this could not be unequivocally shown, and it must be borne in mind that the prediction of Ref. [12] applies to large Stokes numbers in systems with a very well developed inertial range, so that the scale-dependent Stokes number at the largest scale is much less than unity. These questions remain for further studies.

Dissipation-range theory [6, 14–16, 21] predicts how the relative-velocity fluctuations depend on particle separation. This power-law dependence of the relative-velocity moments upon particle separation is universal (but the prefactors of the power laws are not). The original inertial-range theories discussed above do not refer to particle separations in the dissipation range, and attempts to modify inertial-range theories to take into account dissipation-range dynamics [57, 58] were shown to fail (Fig. 5 in Ref. [13]), so that they cannot be used to model collision velocities of microscopic dust grains in circumstellar accretion disks, where collisions happen in the dissipation range. It is challenging to use DNS to determine collision rates and velocities of small grains deep in the dissipation range, because such encounters are infrequent, yet significant. Usually, DNS data on relative-particle velocities [13, 17, 53] are evaluated at fixed separations of order  $\eta$ , as discussed above. The theory described and tested here allows to extrapolate the

DNS results to the relevant scales, often much smaller than the Kolmogorov length  $\eta$ .

Note that Eq. (18) is essentially an expansion in powers of  $St_2$  for small  $St_2$  where we have retained terms up to first order in  $St_2$ . We have checked from our DNS that the correlation function on the second lines of Eq. (18) is always negative and is proportional to  $St_1^2$  for small  $St_1$ . Eq. (18), which is confirmed by our DNS, (Fig. (3) (c)), is clearly in disagreement with Abrahamson’s theory [59] which predicts that the rms relative velocity of two inertial particles is given by the sum of their individual rms velocities. This disagreement becomes apparent if we take the limit  $St_2 \rightarrow 0$  in Eq. (18) in which case the rms relative velocity appears as *difference* between the rms velocities of an inertial particle and a tracer. This is because Ref. [59] assumes that the motion of the two particles are uncorrelated – an approximation of dubious

validity when the particles are close to each other, i.e., about to collide. This again illustrates one of the central messages of this paper: a theory of relative velocity of two particles must take into account the distance between them, otherwise the theory will fail to predict collision velocities.

## VII. ACKNOWLEDGMENTS

This work is supported by the grant Bottlenecks for particle growth in turbulent aerosols from the Knut and Alice Wallenberg Foundation (Dnr. KAW 2014.0048), by Vetenskapsradet [grants 2013-3992 and 2017-03865], and Formas [grant number 2014-585]. The computations were performed on resources provided by the Swedish National Infrastructure for Computing (SNIC) at PDC. DM and AB thank John Wettlaufer for useful discussions.

- 
- [1] HR Pruppacher and JD Klett, *Microphysics of Clouds and Precipitation*, Vol. 18 (Springer Science & Business Media, 2010).
  - [2] M. Wilkinson, B. Mehlig, and V. Uski, “Stokes trapping and planet formation,” *Astrophys. J. Suppl.* **176**, 484–496 (2008).
  - [3] P. J. Armitage, *Astrophysics of Planet Formation* (Cambridge University Press, Cambridge, UK, 2010).
  - [4] A. Johansen, J. Blum, H. Tanaka, C. Ormel, M. Bizzaro, and H. Rickman, in *Protostars & planets VI*, edited by H. Beuther, R. S. Klessen, C. P. Dullemond, and T. Henning (University of Arizona Press, 2014).
  - [5] S. J. Weidenschilling and J. N. Cuzzi, “Formation of planetesimals in the solar nebula,” in *Protostars and Planets III* (Univ. of Arizona Press, Tucson, 1993) p. 1031.
  - [6] K Gustavsson and B Mehlig, “Relative velocities of inertial particles in turbulent aerosols,” *Journal of Turbulence* **15**, 34–69 (2014).
  - [7] F. Windmark, T. Birnstiel, C. W. Ormel, and C. P. Dullemond, “Breaking through: The effects of a velocity distribution on barriers to dust growth,” *A & A* **544**, L16 (2012).
  - [8] HJ Völk, FC Jones, GE Morfill, and S Roeser, “Collisions between grains in a turbulent gas,” *Astronomy and Astrophysics* **85**, 316–325 (1980).
  - [9] H. Mizuno, WJ Markiewicz, and HJ Völk, “Grain growth in turbulent protoplanetary accretion disks,” *Astronomy and Astrophysics* **195**, 183–92 (1988).
  - [10] WJ Markiewicz, H Mizuno, and HJ Völk, “Turbulence induced relative velocity between two grains,” *Astronomy and Astrophysics* **242**, 286–289 (1991).
  - [11] Bernhard Mehlig, Ville Uski, and Michael Wilkinson, “Colliding particles in highly turbulent flows,” *Physics of Fluids* **19**, 098107 (2007).
  - [12] K. Gustavsson, B. Mehlig, M. Wilkinson, and V. Uski, “Variable-range projection model for turbulence-driven collisions,” *Phys. Rev. Lett.* **101** (2008), 174503.
  - [13] Takashi Ishihara, Naoki Kobayashi, Kei Enohata, Masayuki Umemura, and Kenji Shiraishi, “Dust coagulation regulated by turbulent clustering in protoplanetary disks,” *The Astrophysical Journal* **854**, 81 (2018).
  - [14] K Gustavsson and B Mehlig, “Distribution of relative velocities in turbulent aerosols,” *Physical Review E* **84**, 045304 (2011).
  - [15] K. Gustavsson, E. Meneguz, M. Reeks, and B. Mehlig, “Inertial-particle dynamics in turbulent flows: caustics, concentration fluctuations, and random uncorrelated motion,” *New. J. Phys.* **14** (2012), 115017.
  - [16] K Gustavsson and B Mehlig, “Statistical model for collisions and recollisions of inertial particles in mixing flows,” *Eur. Phys. J. E* **39**, 55 (2016).
  - [17] Liubin Pan and Paolo Padoan, “Turbulence-induced relative velocity of dust particles. I. Identical particles,” *The Astrophysical Journal* **776**, 12 (2013).
  - [18] Liubin Pan, Paolo Padoan, and John Scalo, “Turbulence-induced relative velocity of dust particles. iii. the probability distribution,” *The Astrophysical Journal* **792**, 69 (2014).
  - [19] Vincent E Perrin and HJJ Jonker, “Relative velocity distribution of inertial particles in turbulence: A numerical study,” *Physical Review E* **92**, 043022 (2015).
  - [20] Akshay Bhatnagar, K Gustavsson, and Dhruvadya Mitra, “Statistics of the relative velocity of particles in turbulent flows: Monodisperse particles,” *Physical Review E* **97**, 023105 (2018).
  - [21] J Meibohm, L Pistone, K Gustavsson, and B Mehlig, “Relative velocities in bidisperse turbulent suspensions,” *Physical Review E* **96**, 061102 (2017).
  - [22] Ewe-Wei Saw, Gregory P. Bewley, Eberhard Bodenschatz, Samriddhi Sankar Ray, and Jeremie Bec, “Extreme fluctuations of the relative velocities between droplets in turbulent airflow,” *Physics of Fluids* **26**, 111702 (2014).
  - [23] Zhongwang Dou, Andrew D Bragg, Adam L Hammond, Zach Liang, Lance R Collins, and Hui Meng, “Effects of reynolds number and stokes number on particle-pair relative velocity in isotropic turbulence: a systematic experimental study,” *Journal of Fluid Mechanics* **839**, 271–292

- (2018).
- [24] J. Chun, D. L. Koch, S. L. Rani, A. Ahluwalia, and L. R. Collins, “Clustering of aerosol particles in isotropic turbulence,” *J. Fluid Mech.* **536**, 219–251 (2005).
- [25] J. Bec, A. Celani, M. Cencini, and S. Musacchio, “Clustering and collisions in random flows,” *Phys. Fluids* **17** (2005), 073301.
- [26] K. Gustavsson and B. Mehlig, “Statistical models for spatial patterns of heavy particles in turbulence,” *Advances in Physics* **65**, 1–57 (2016).
- [27] A. Brandenburg and W. Dobler, “Hydromagnetic turbulence in computer simulations,” *Computer Physics Communications* **147**, 471–475 (2002).
- [28] JH Williamson, “Low-storage runge-kutta schemes,” *Journal of Computational Physics* **35**, 48–56 (1980).
- [29] A. Brandenburg, “The inverse cascade and nonlinear alpha-effect in simulations of isotropic helical hydromagnetic turbulence,” *The Astrophysical Journal* **550**, 824–840 (2001).
- [30] D.J. Higham, “An algorithmic introduction to numerical simulations of stochastic differential equations.” *SIAM Review* **43**, 525–546 (2001).
- [31] Wolfgang Dobler, Nils Erland L Haugen, Tarek A Yousef, and Axel Brandenburg, “Bottleneck effect in three-dimensional turbulence simulations,” *Physical Review E* **68**, 026304 (2003).
- [32] Nils Erland L Haugen, Axel Brandenburg, and Wolfgang Dobler, “Is nonhelical hydromagnetic turbulence peaked at small scales?” *The Astrophysical Journal Letters* **597**, L141 (2003).
- [33] Nils Erland L. Haugen and Axel Brandenburg, “Inertial range scaling in numerical turbulence with hyperviscosity,” *Phys. Rev. E* **70**, 026405 (2004).
- [34] Raymond A Shaw, “Particle-turbulence interactions in atmospheric clouds,” *Annual Review of Fluid Mechanics* **35**, 183–227 (2003).
- [35] P. S. Epstein, “On the resistance experienced by spheres moving through gases,” *Phys. Rev.* **23**, 710 (1924).
- [36] G Falkovich, A Fouxon, and MG Stepanov, “Acceleration of rain initiation by cloud turbulence,” *Nature* **419**, 151–154 (2002).
- [37] M Wilkinson and Bernhard Mehlig, “Caustics in turbulent aerosols,” *Europhys. Lett.* **71**, 186 (2005).
- [38] Michael Wilkinson, Bernhard Mehlig, and Vlad Bezuglyy, “Caustic activation of rain showers,” *Physical review letters* **97**, 048501 (2006).
- [39] Michel Voßkuhle, Alain Pumir, Emmanuel Lévêque, and Michael Wilkinson, “Prevalence of the sling effect for enhancing collision rates in turbulent suspensions,” *Journal of Fluid Mechanics* **749**, 841–852 (2014).
- [40] J. Bec, L. Biferale, M. Cencini, A. Lanotte, and F. Toschi, “Intermittency in the velocity distribution of heavy particles in turbulence,” *J. Fluid Mech.* **646**, 527–536 (2010).
- [41] J. Bec, L. Biferale, M. Cencini, A. Lanotte, and F. Toschi, “Spatial and velocity statistics of inertial particles in turbulent flows,” *Journal of Physics: Conference Series* **333**, 012003 (2011).
- [42] J. P. L. C. Salazar and L. R. Collins, “Inertial particle relative velocity statistics in homogeneous isotropic turbulence,” *JFM* **696**, 45–66 (2012).
- [43] Martin James and Samriddhi Sankar Ray, “Enhanced droplet collision rates and impact velocities in turbulent flows: The effect of poly-dispersity and transient phases,” *Scientific Reports* **7**, 12231 (2017).
- [44] Jeremie Bec, Luca Biferale, Massimo Cencini, A Lanotte, Stefano Musacchio, and Federico Toschi, “Heavy particle concentration in turbulence at dissipative and inertial scales,” *Physical review letters* **98**, 084502 (2007).
- [45] M. Wilkinson, B. Mehlig, and K. Gustavsson, “Correlation dimension of inertial particles in random flows,” *Europhys. Lett.* **89** (2010), 50002.
- [46] K. Gustavsson, B. Mehlig, and M. Wilkinson, “Analysis of the correlation dimension of inertial particles,” *Phys. Fluids* **27** (2015), 073305.
- [47] K. Gustavsson and B. Mehlig, “Distribution of velocity gradients and rate of caustic formation in turbulent aerosols at finite Kubo numbers,” *Phys. Rev. E* **87** (2013), 023016.
- [48] Jeremy Bec, Luca Biferale, Guido Boffetta, Antonio Celani, Massimo Cencini, Alessandra Lanotte, S Musacchio, and Federico Toschi, “Acceleration statistics of heavy particles in turbulence,” *Journal of Fluid Mechanics* **550**, 349–358 (2006).
- [49] Akshay Bhatnagar, *Direct Numerical Simulations of Fluid Turbulence: (A) Statistical Properties of Tracer and Inertial Particles (B) Cauchy-Lagrange Studies of the Three-Dimensional Euler Equation*, Ph.D. thesis, Dept. of Physics, Indian Institute of Science, Bangalore. (2016).
- [50] This agreement should be understood in the following manner. The theory does not allow a calculation of  $\mu_c$  from first principle, but it shows that  $\mu_c = D_2(\overline{St})$  for small  $\theta$ . This is indeed what we confirm from DNS.
- [51] Rohit Dhariwal and Andrew D Bragg, “Small-scale dynamics of settling, bidisperse particles in turbulence,” *Journal of Fluid Mechanics* **839**, 594–620 (2018).
- [52] This can be derived using the Kolmogorov scaling  $u_{rms}/u_\eta \sim (l_f/\eta)^{1/3}$ , where  $l_f = 1/k_f$  is forcing scale.
- [53] Liubin Pan, Paolo Padoan, and John Scalo, “Turbulence-induced relative velocity of dust particles. II. The bidisperse case,” *The Astrophysical Journal* **791**, 48 (2014).
- [54] Leonid I Zaichik, Olivier Simonin, and Vladimir M Alipchenkov, “Two statistical models for predicting collision rates of inertial particles in homogeneous isotropic turbulence,” *Physics of Fluids* **15**, 2995 (2003).
- [55] Leonid I Zaichik, Vladimir M Alipchenkov, and Emmanuil G Sinaiski, *Particles in turbulent flows* (John Wiley & Sons, 2008).
- [56] Liubin Pan and Paolo Padoan, “Relative velocity of inertial particles in turbulent flows,” *Journal of Fluid Mechanics* **661**, 73–107 (2010).
- [57] CW Ormel and JN Cuzzi, “Closed-form expressions for particle relative velocities induced by turbulence,” *Astronomy & Astrophysics* **466**, 413–420 (2007).
- [58] Liubin Pan and Paolo Padoan, “Turbulence-induced Relative Velocity of Dust Particles V. Testing Previous Models,” *The Astrophysical Journal* **812**, 10 (2015).
- [59] J Abrahamson, “Collision rates of small particles in a vigorously turbulent fluid,” *Chemical Engineering Science* **30**, 1371–1379 (1975).